https://dx.doi.org/10.1016/j.jcsr.2019.07.012

NONLINEAR FINITE-ELEMENT-ANALYSIS AND DESIGN OF STEEL-CONCRETE COMPOSITE RING (SCCR) JOINTS

Liang Chen, Si-Wei Liu*, Chi-Kin Lau and Siu-Lai Chan

Author Affiliations:

[1]*Post-graduate Student, Department of Civil and Environmental Engineering, The Hong Kong Polytechnic University, Hung Hom, Kowloon, Hong Kong, China, E-mail: liang17.chen@connect.polyu.hk*

[2]*Associate Professor, School of Civil Engineering, Sun-Yat-Sen University, No. 135, Xingang Xi Road, Guangzhou, 510275, China,* ***(corresponding author)*** *E-mail: Liusw8@mail.sysu.edu.cn*

[3]*Chief Structural Engineer,* Sun Hung Kai Architects and Engineers Ltd., Hong Kong, China, *E-mail: cklau@shkp.com*

[4]*Chair Professor, Department of Civil and Environmental Engineering, The Hong Kong Polytechnic University, Hung Hom, Kowloon, Hong Kong, China, E-mail: ceslchan@polyu.edu.hk*

Abstract

Conventional steel-plates-strengthened-composite ring (SPSC) joints are extensively used in composite structures to connect concrete-filled tubular (CFT) columns and reinforced concrete (RC) beams. However, the refinancing-bars of the adjacent beams require on-site welding to the steel strengthened plates of the SPSC joint, which, regarding workmanship, is difficult and time-consuming. Recently, a new type of joint, the steel-concrete-composite-ring (SCCR) joint, has been proposed as a substitute for the SPSC joint since it has been successfully used in several construction projects in Hong Kong. An SCCR joint consists of a steel tube, a concrete ring beam with reinforcements in both the radial and hoop directions, and shear studs. This research develops a sophisticated Finite-Element (FE) modelling method for SCCR joints, where the dominant factors affecting the joint's behaviors are considered, such as the explicit simulation of the complex reinforced bar details and shear studs, the cracking and crushing of concrete, the yielding of reinforced bars, and the contact behaviors between the steel tube and the concrete. From the FE analysis results, four possible failure modes are identified. Parametric studies are sequentially conducted in regard to these modes, yielding corresponding design equations. A design procedure developed through the proposed equations is illustrated with a flowchart. Finally, a real-world example project is presented and further validated by sophisticated FE analysis.

Keywords: *Finite Element Method, Composite Joint, Nonlinear, Design, Analysis, Concrete*

1 Introduction

Concrete-filled tubular (CFT) columns are commonly used in various types of modern construction projects due to their strength, stiffness, and excellent ductility, among other qualities [1-3]. The main difficulty in adopting this type of structure pertains to the connection between reinforced concrete (RC) beams and CFT columns. The reinforcement bars within RC beams cannot be directly attached to the CFT column due to the steel tube. Therefore, a steel-plate-strengthened-composite ring (SPSC) joint, as shown in Figure 1 (a), is conventionally employed. These require the reinforcement bars of the RC beams to be welded to the steel strengthened plates on-site, a difficult and time-consuming process. Recently, a new method for connection, the steel-concrete-composite-ring (SCCR) joint (Figure 1 (b)), has been proposed as a substitute for the traditional SPSC joints after having been successfully used in several construction projects in Hong Kong (see Figure 2). In the SCCR joint, the CFT column and the RC beams are connected by an RC ring beam, eliminating the challenge of on-site welding.

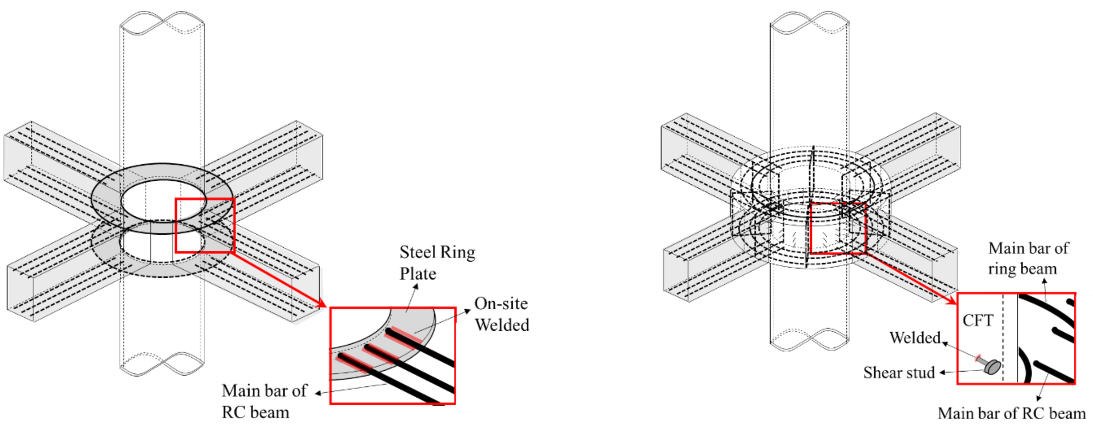

(a) SPSC joint (b) SCCR joint

Figure 1 The composite joints connecting RC beams and the CFT column

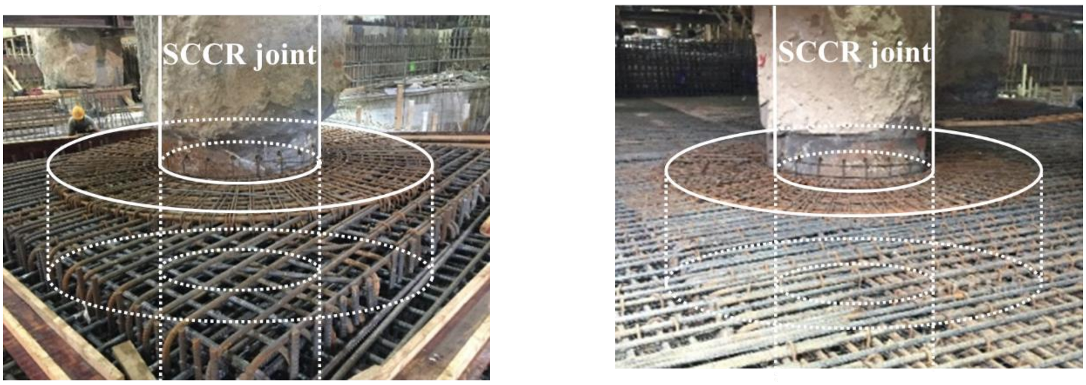

Figure 2 A real case application of the SCCR joint

The study of composite joints has become popular among researchers. Schneider and Alostaz [4] analyzed the connection of the steel strengthened plate within the steel beam to the CFT column (SBCC) joint through experiment-based investigations and Finite-Element Analysis (FEA). Elremaily and Azizinamini [5] presented a design process for the SBCC joint also with the aid of the Finite-Element (FE) model. Later, other researchers (such as Cheng and Chung [6], Ricles *et al.* [7], and Sheet *et al*. [8],) further investigated the performance of the SBCC joint under cyclic loading. Furthermore, Azizinamini [9] *et al*. proposed a series of equations for the design of through-beam connections, wherein the steel tube is cut off to maintain the continuity of the beam. Tang *et al*. [10] studied the seismic performance of the through-beam connection using the FEA approach, whereas Nie *et al*. [11, 12] introduced a new connection system for CFT columns and beams which used a rectangular, steel stiffening ring inside the joints. Later, Zhang *et al*. [13] studied the seismic behavior of this connection system. However, despite the aforementioned studies, related research specifically on the SCCR joint is still relatively limited.

Eurocode 3-1-8 [14] provides a modern joint design process based on failure modes, comprehensively considering the strength, stiffness, and deformation of a joint. This method has been adopted by a number of researchers. For example, Bijlaard [15] provided an overview of the design philosophy and emphasized that reliable software tools can make the use of the Eurocodes easier for engineers. In addition, D'Aniello *et al*. [16] investigated the seismic design of extended stiffened end-plate joints in the framework of Eurocodes. El-Khoriby *et al*. [17] employed the FE model to propose a series of design recommendations for the beam-to-column connection under axial forces and cyclic bending moments.

By studying the structural performance of SCCR joints and identifying possible failure modes, this paper adopts the FEA method to establish a sophisticated model for investigating the performance of the joints under different loads. The FEA method is commonly considered one of the most reliable numerical approaches for examining structural behaviors. Indeed, several researchers have adopted the FEA method for their studies. For example, Tang *et al*. [10] studied the seismic performance of the composite connection using the FEA approach, their results being validated by conducted experiments. Furthermore, Subramani [18] *et al*. investigated deflection and energy absorption capacities of the retrofitted RC beam-column joints also using the FEA method. Ramadan *et al*. [19], Ouyang *et al*. [20, 21] and Pagoulatou *et al*. [22] proposed employing the FE model for the examination of CFT columns under different loads, with numerical simulation results being in-line with experimental observations. In this paper, four possible failure modes are identified from the FEA results, and consequently, the design equations for computing the SCCR joint's strength capacities in regard to these failure modes are derived from parametric studies. To verify the accuracy of the design equations, hand-calculated results are compared to those from the FEA. Finally, a design example from a real-world project that use the proposed equations for the design process is presented.

2 Finite-Element (FE) Modelling

A sophisticated FE model is developed to predict the performance of the SCCR joint and identify the possible failure modes for the further conduction of the parametric studies. As presented in Figure 3, the SCCR joint is composed of reinforcements, concrete, a steel tube, and shear links. This paper employs FEA software ANSYS (14.0) to simulate the SCCR joint.

In the FE model, the dominant factors affecting the joint's performance are considered, such as the cracking and crushing of concrete, the yielding of steel, the explicit modelling of the complex reinforcement bar details, and the contact behaviors between the steel tube and the concrete. Detailed information regarding the FE model is further presented in the following sections.

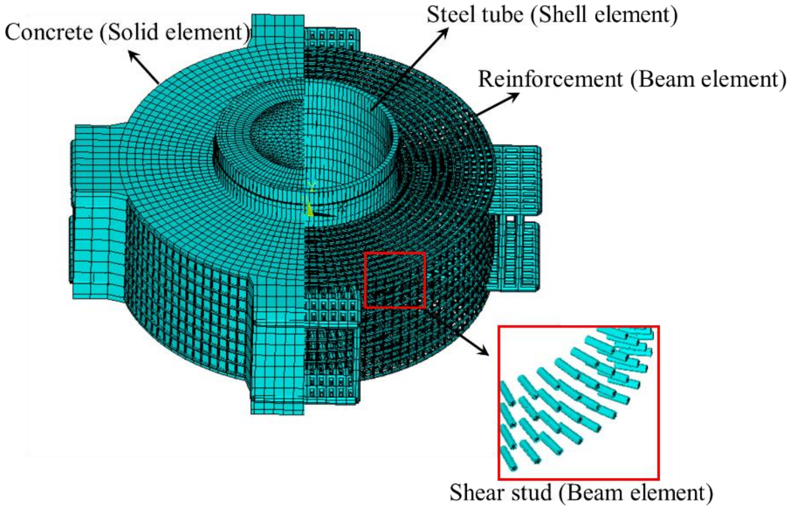

Figure 3 Finite-Element (FE) model of the SCCR joint

2.1 Assumptions

The following assumptions are adopted: (1) there is no slippage between the concrete and reinforcement components; (2) full composite actions can be developed between the steel tube and the concrete component; (3) the RC beam and CFT column are designed with adequate strength for enduring external loads; (4) only compression-action exists between the steel tube and concrete component areas of contact; and (5) there is no friction between the steel tube and RC ring beam contact areas, and all shear forces are transferred by shear studs.

2.2 Finite-Element Modelling of the Basic Components

2.2.1 Concrete

An eight-node solid element with three degrees of freedom at each node is employed to discretize the concrete component of the SCCR joint. The element is an advanced 3-D element which adopts the Willama and Warnke model [15], and it can simulate the cracking, crushing, plastic deformation, and creep behaviors of concrete. In the present study, the uniaxial tensile cracking stress of concrete is taken as 0.1 times that of the uniaxial crushing stress, and the shear transfer coefficients of the concrete for the open crack and closed crack are set as 0.95 and 1.0, respectively. Generally, a mesh size equalling 0.05 to 0.1 times of the ring beam width is adopted, whereas the concrete core of the CFT column is free-meshed by the software (Figure 3).

2.2.2 Reinforcement and Steel Tube

In the proposed FE model, the stress–strain relationship of the steel components (i.e. both the reinforcements and the steel tube) is assumed to be elastic-perfectly-plastic, which can be expressed as:

$$\sigma_s = E_s \varepsilon_s \ \text{for} \ -\varepsilon_{fy} < \varepsilon_s < \varepsilon_{fy} \tag{1}$$

$$\sigma_s = f_{yd} \ \text{for} \ \varepsilon_s < -\varepsilon_{fy} \ \text{or} \ \varepsilon_s > \varepsilon_{fy} \tag{2}$$

where, E_s is the Young's modulus, f_{yd} represents the yield strength, and ε_{fy} is the corresponding strain.

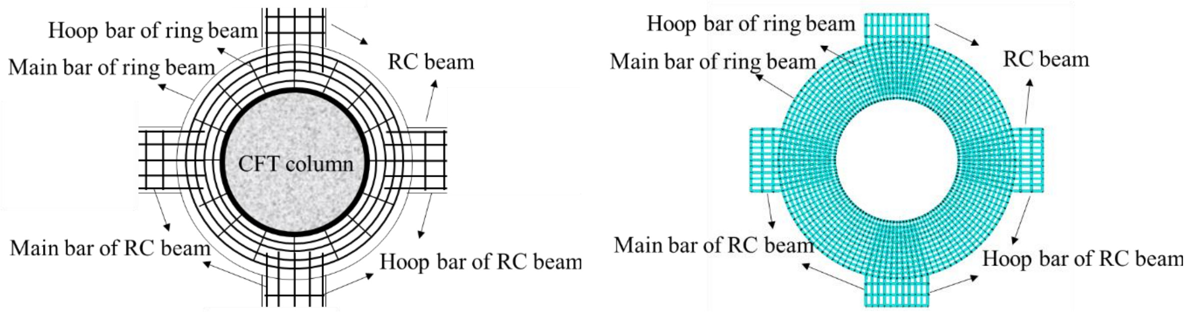

Figure 4 The FE modelling of the reinforcements using beam elements

The reinforcements of the SCCR joint are simulated by beam elements with six degrees of freedom at each node. The beam element is based on Timoshenko beam theory [23, 24] which includes shear-deformation effects and is suitable for linear, large rotation, and large strain nonlinear applications. All the reinforcements of the SCCR joint (i.e., main bars, hoop bars, side bars, etc.) are modelled by beam elements and meshed accordingly, with the distributions of the beam elements based on the design details of the joint (Figure 4). This paper assumes that there is no slippage between the concrete and reinforcement components; thus, the interactions between them can be simply simulated by sharing the element nodes at the contact surfaces.

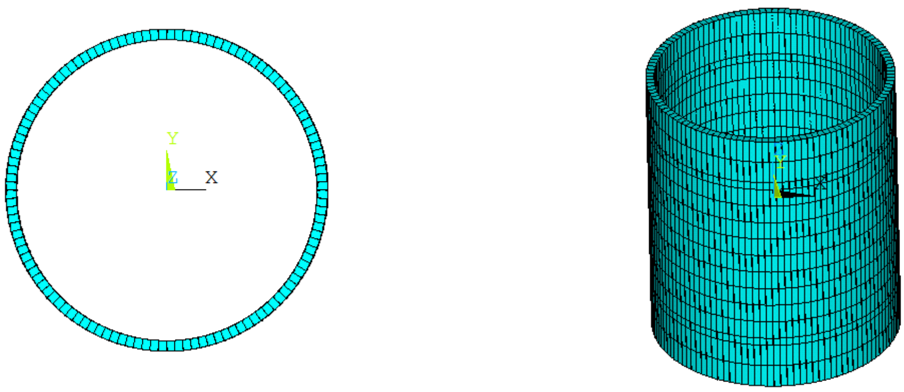

Figure 5 The FE modelling of the steel tube using shell elements

As shown in Figure 5, the steel tube of the CFT column is simulated using shell elements with six degrees of freedom at each node. The four-node shell element adopted in this paper possesses plasticity, stress stiffening, large deflection, and large strain capabilities. To ensure the ease of modelling the contact surfaces (see the next section), all shell elements are rectangular and uniformly distributed along the perimeter of the column.

2.2.3 Contact Surfaces Between the Steel Tube and Ring Beam

In the modelling of the SCCR joint, the simulation of the contact surfaces between the steel tube and reinforced ring beam is essential. This research discretizes the contact surfaces via a series of contact pairs. As shown in Figure 6, a contact pair is composed of one steel tube element node, one ring beam element node, and a compression-only link element connecting these two nodes. The link element is of negligible length, and the cross-sectional area is calculated accordingly. To transfer the compression force directly, the link elements require a high level of stiffness. Thus, the Young’s modulus of the link element is set as ten times that of the steel element.

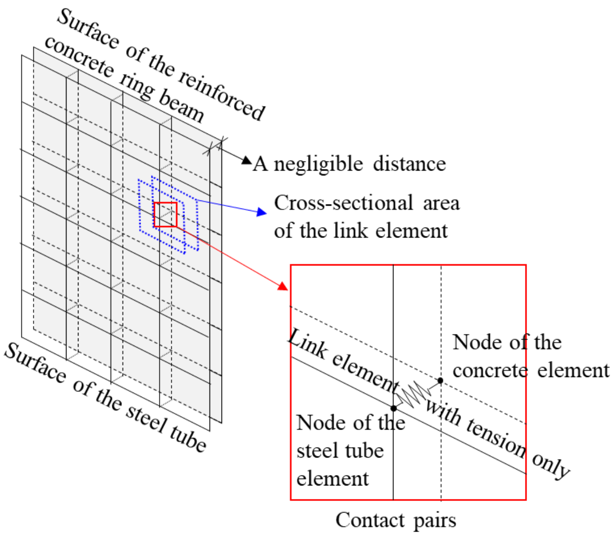

Figure 6 Contact pairs

2.2.4 Shear Studs

In the present research, the proposed FE model adopted shear studs to transfer the shear forces from the ring beam to the CFT column. Several researchers have studied the capacities of shear studs. For example, Johnson and May [25] recommended that the stiffness of shear studs should be taken as the tangent stiffness at half of the maximum shear capacity, and Eurocode-4 [26] suggests that the design shear capacity of a shear stud should not exceed more than 0.8 times the maximum. Thus, based on the results presented by Lam *et al*.[27] and Shim *et al*.[28], the present study adopts a bilinear force-slip relationship as shown in in Figure 7, in which P_k is the maximum shear capacity of the shear stud.

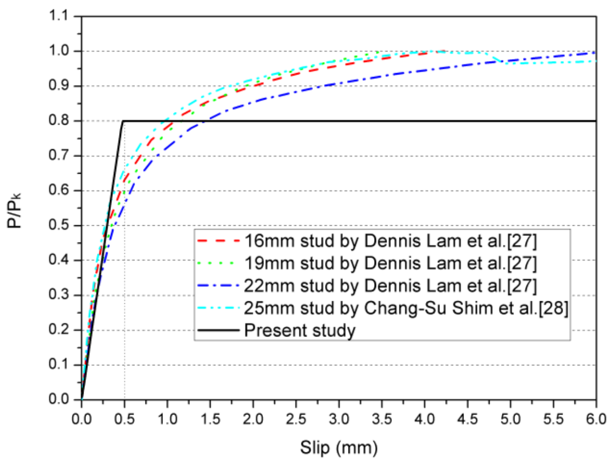

Figure 7 Force-slip relationship of the shear stud

2.3 Failure Modes

According to the modern joint design method [14], the strength, stiffness, and deformation of a joint should be comprehensively considered to identify possible failure modes. This paper adopts the proposed FE models to predict the performance of the SCCR joint. From the FE analysis results, four potential failure modes are identified.

1) Failure Mode A: Bearing crushing of the ring beam concrete

This failure mode occurs when the unbalanced moment (see **Appendix-I**) applied on the SCCR joint is large. The unbalanced moment creates two compressive zones at the top and bottom of the ring beam as shown in Figure 8, with concrete crushing occurring once the bearing stress reaches the failure value. Since the CFT column concrete is confined by the steel tube, the concrete bearing crushing always occurs on the ring beam.

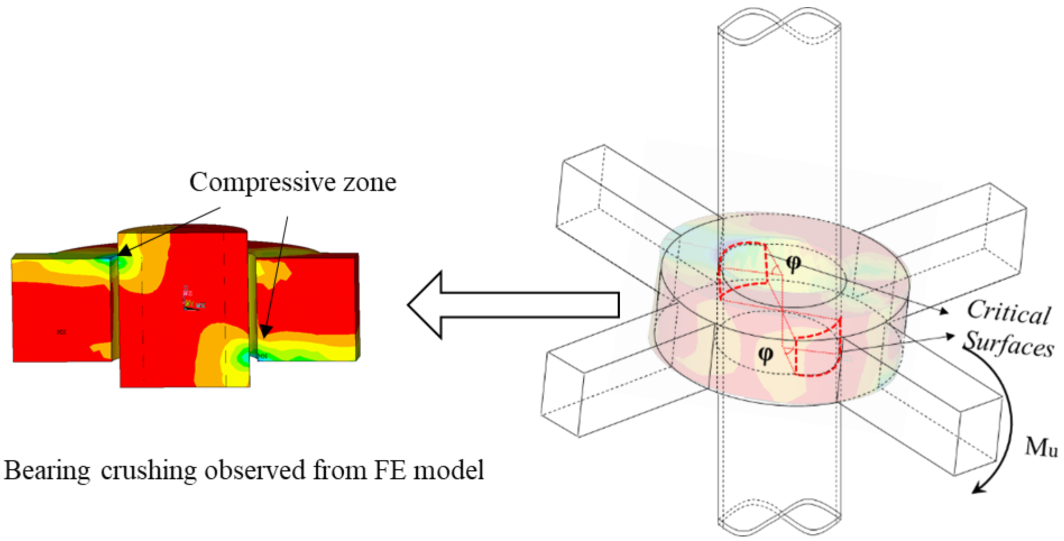

Figure 8 Failure mode A: Bearing crushing of the ring beam concrete

2) Failure mode B: Bending failure of the ring beam

The moment applied on the SCCR joint will induce ring beam tension and compression. The FEA results illustrate that the tensile strength of the concrete has been exceeded, and the concrete of the ring beam cracks. Since tension cannot be transmitted across the crack, the reinforcements on top of the ring beam resist the overall tension, while the concrete at the bottom bears the compression. With bending moment increase, the ultimate strength of the reinforcement bars or concrete will be reached, and the joint will fail via bending failure (Figure 9).

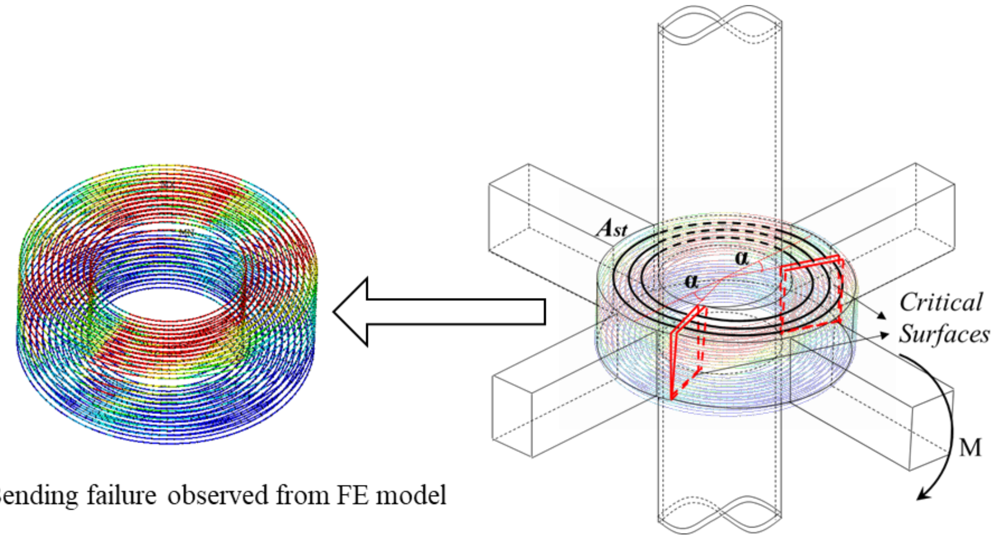

Figure 9 Failure mode B: Bending failure of the ring beam

3) Failure Mode C: Torsional failure of the ring beam

As shown in Figure 10, for a T-shape beam, the bending moment of Beam A will cause a twisting moment on Beam B, and Beam B might fail in torque. A similar failure mode will occur in the SCCR joint if the ring beam does not have enough torsional bearing capacity. A bending moment from the adjacent beam causes shear stresses that results in diagonal tension stresses on the ring beam, with slant cracks appearing under the tension stresses. After cracking, the twisting moment will be carried by the outermost hoop bars and the longitudinal reinforcement located near the surface of the ring beam. The SCCR joint will fail in torsional failure when these torsional-resistance reinforced bars yield.

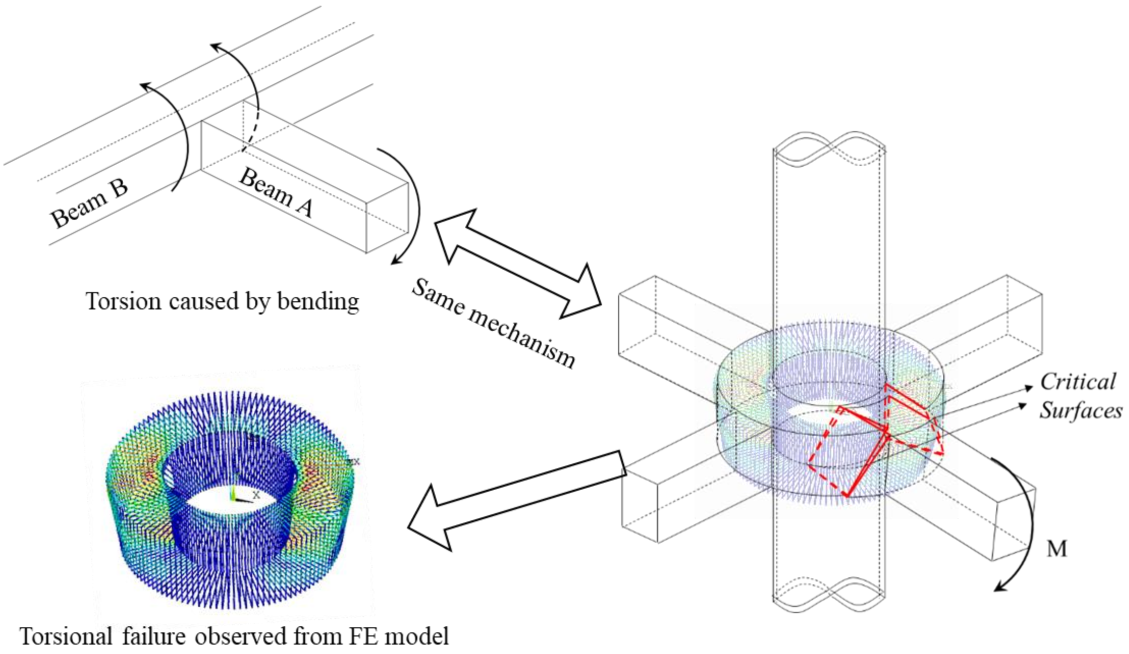

Figure 10 Failure mode C: Torsional failure of the ring beam

4) Failure Mode D: Failure of the shear studs

This paper assumes that there is no friction on the steel tube and ring beam contact areas and that all the shear forces are transferred by shear studs. When the number of shear studs is not high enough and the shear studs cannot bear the shear forces applied on the SCCR joint, the SCCR joint will fail (Figure 11).

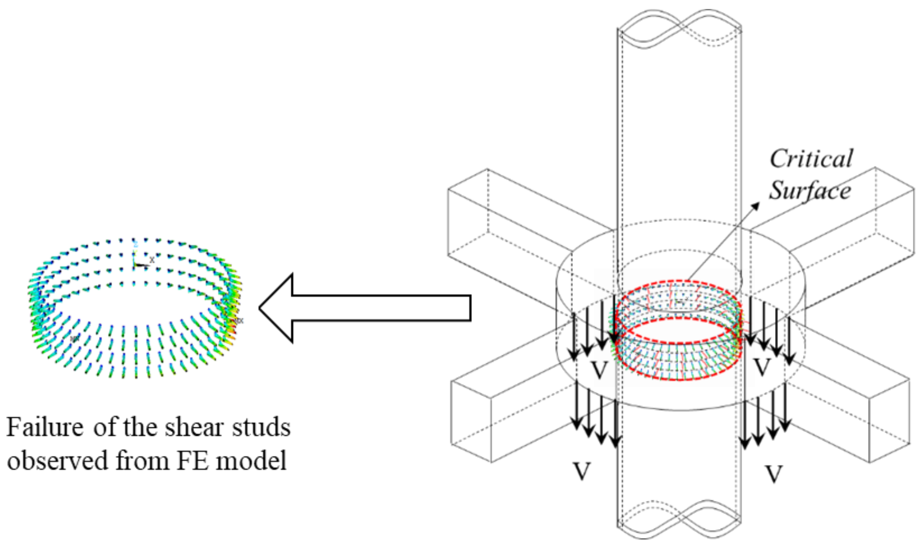

Figure 11 Failure modes D: Failure of the shear studs

3 Design Equations as per the Failure Modes

Based on the aforementioned failure modes, parametric studies are conducted to derive design equations for computing the SCCR joint's strength. This detailed derivation procedure is shown below.

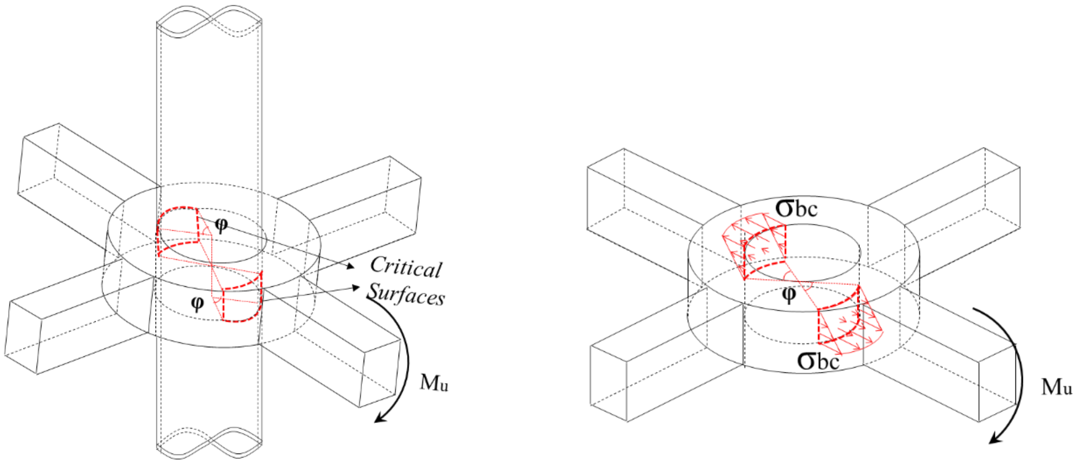

(a) (b)

Figure 12 The SCCR joint failed by bearing crushing of the ring beam concrete

3.1 Failure Mode A - Bearing Crushing of the Ring Beam Concrete

If the applied unbalanced moment is large, the SCCR joint will fail due to the crushing of the ring beam concrete as shown in Figure 12(a). From the FEA results, the stress distribution on the critical surfaces before the concrete crushes can be simplified (Figure 12b), and the resistance moment can be calculated by:

$$M_u = \frac{\varphi \pi \mathrm{D}_d}{2} \frac{\sigma_{bc}}{2} \frac{r_h}{2} \frac{2r_h}{3} \tag{3}$$

in which, r_h is the depth of the concrete ring beam, D_d is the diameter of the column, σ_{bc} is the concrete bearing strength, and $\varphi\pi D_d/2$ is the equivalent width of the crushing area as shown in Figure 12(b). According to the parametric studies, the coefficient φ can be taken as 0.6 for general cases.

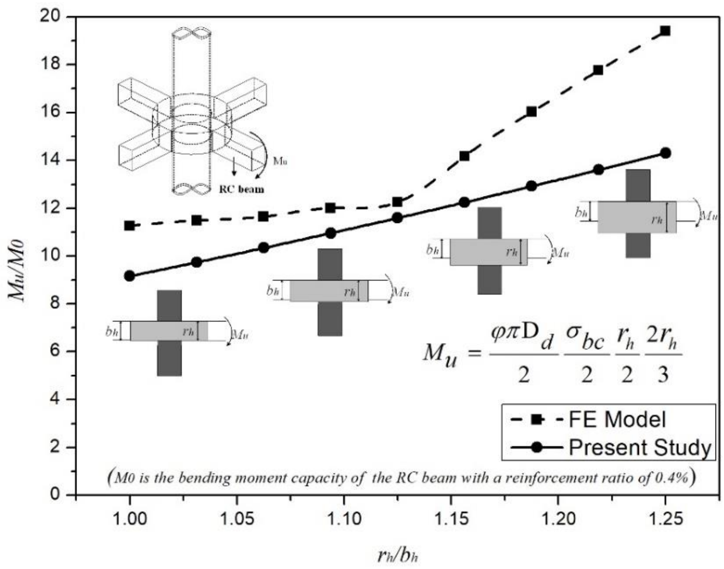

Figure 13 Results from the FE model and the proposed design equation for failure mode A

To check the accuracy of equation (3), the moment capacities of the joint with different heights are calculated by the FEA method and the proposed equation. The results are plotted in Figure 13.

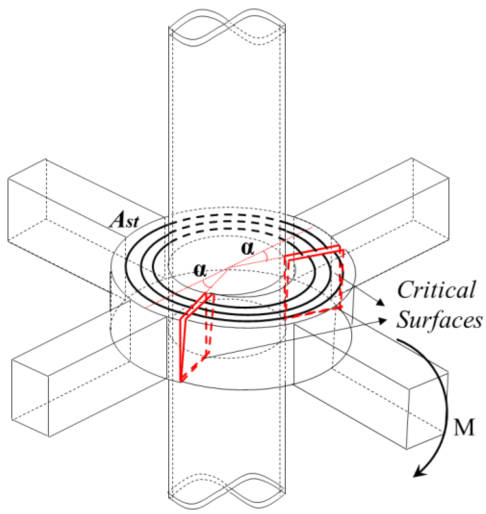

Figure 14 Bending failure of the ring beam

3.2 Failure Mode B - Bending Failure of the Ring Beam

To resist the bending moment, the reinforcements at the top of the ring beam will be under tension while the concrete at the bottom will bear the compression. The bending failure of the joint will occur when the maximum strength of the reinforcement bars or concrete is reached, as shown in Figure 14. From the FEA results, the stress and strain distributions on the critical surfaces in this failure mode can be simplified as shown in Figure 15.

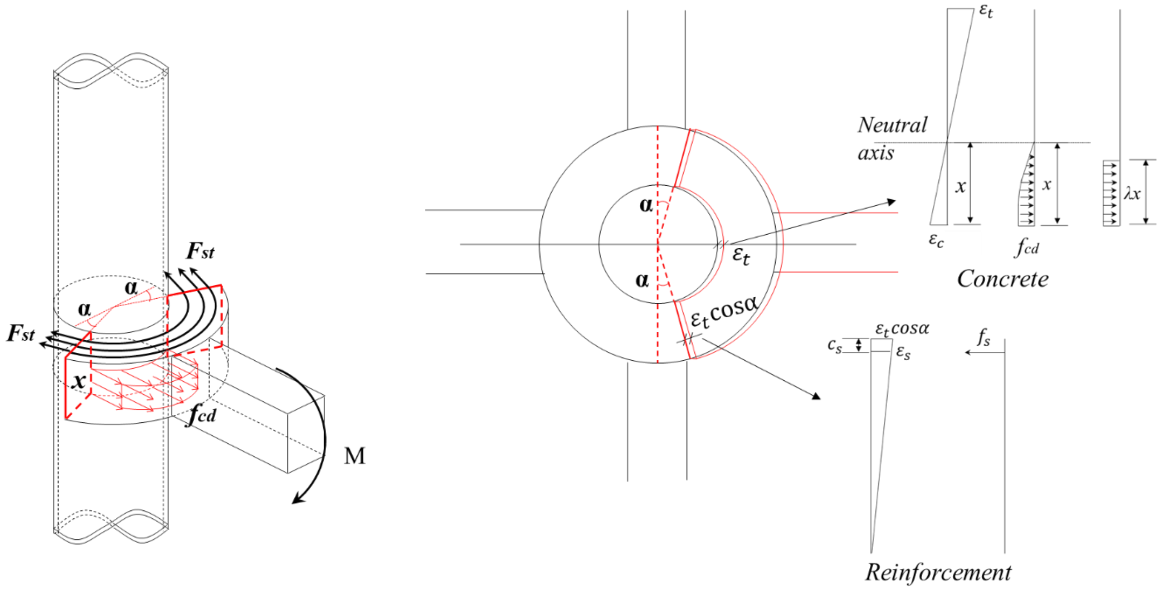

(a) (b)

Figure 15 The stress and strain distributions on the critical surfaces of failure mode B

From Figure 15(b), the relationship between the maximum concrete strain ε_c and the average strain of reinforcements ε_s can be computed by:

$$\frac{\varepsilon_c}{x} = \frac{\varepsilon_t}{r_h - x} \tag{4}$$

$$\frac{\varepsilon_s}{r_h - c_s} = \frac{\varepsilon_t \cos\alpha}{r_h} \tag{5}$$

where x is the depth of the neutral axis, ε_t is the tensile strain at the top of the ring beam, c_s is the distance from the center of the reinforcements to the top of the concrete ring beam, and $\alpha=30^o$ is the intersection angle between the critical surface and the symmetry axis of the SCCR joint given by the FEA results.

Conventionally, the ring beam depth r_h is far larger than the distance from the center of the reinforcements to the top of the concrete ring beam c_s; so that equation (5) can be simplified as:

$$\varepsilon_s = \varepsilon_t \cos\alpha \tag{6}$$

The FEA results indicate that the SCCR joints have two bending failure modes: *Primary Tension Failure* (concrete is crushed after the reinforcements yield) and *Primary Compression Failure* (concrete is crushed before the reinforcements yield). The critical moment between them can be calculated by assuming the concrete and the reinforcements fail at the same time:

$$\frac{\varepsilon_{cu}}{x} = \frac{\varepsilon_t}{r_h - x} \tag{7}$$

$$\frac{\varepsilon_{fy}}{r_h - c_s} = \frac{\varepsilon_t \cos\alpha}{r_h} \tag{8}$$

where ε_{cu} is the failure strain of concrete and ε_{fy} is the yielding strain of the reinforcement. The equilibrium equations can be written as:

$$F_c = D_d \cos\alpha \lambda x f_{cd} \tag{9}$$

$$M_{cr} = F_c \left(r_h - c_s - \frac{\lambda x}{2} \right) \tag{10}$$

where λ is the coefficient for the equivalent rectangular stress block and f_{cd} is the failure stress of concrete.

By substituting equation (7), (8) and (9) to (10), it yields the critical moment:

$$M_{cr} = D_d \cos\alpha f_{cd} \lambda x \left(rh - c_s - \frac{\lambda x}{2} \right) \tag{11}$$

in which, $x = \frac{\varepsilon_{cu} \cos\alpha}{\varepsilon_{fy} + \varepsilon_{cu} \cos\alpha} r_h$ is the depth of the neutral axis.

3.2.1 Primary Tension Failure

When the moment applied on the SCCR joint is smaller than the critical moment M_{cr}, the bending failure modes demonstrate *Primary Tension Failure* (concrete crushed after the reinforcements yield), with the force equilibrium equations on the critical surfaces written as:

$$\textit{Compression force:} \qquad F_c = D_d \cos\alpha \lambda x f_{cd} \tag{12}$$

$$\textit{Tension force:} \qquad F_{st} = 2A_{st} f_{yd} \tag{13}$$

$$\textit{The balance of forces:} \qquad F_c = F_{st} \cos\alpha \tag{14}$$

$$\textit{The balance of moments:} \qquad M = F_c \left(r_h - c_s - \frac{\lambda x}{2} \right) \tag{15}$$

where, f_{yd} is the yield strength of reinforcements and A_{st} is the required reinforcement area, which can be computed by solving the force equilibrium equations above:

$$A_{st} = \frac{-2\upsilon + \sqrt{(2\upsilon)^2 - 8M\omega}}{-4\omega} \tag{16}$$

in which, $\upsilon = f_{yd} \cos\alpha \left(r_h - c_s \right)$, $\omega = \dfrac{f_{yd}{}^2 \cos\alpha}{D_d f_{cd}}$

The depth of the neutral axis in this case is:

$$x = \frac{2A_{st} f_{yd}}{\lambda D_d f_{cd}} \tag{17}$$

3.2.2 Primary Compression Failure

If the moment applied on the SCCR joint is larger than the critical moment M_{cr}, the bending failure modes demonstrate *Primary Compression Failure* (concrete crushed before the reinforcements yield), with the force equilibrium equations on the critical surfaces written as:

$$\textit{Compression force:} \qquad F_c = D_d \cos\alpha \lambda x f_{cd} \tag{18}$$

$$\textit{Tension force:} \qquad F_{st} = 2A_{st} E_s \varepsilon_s \cos\alpha \tag{19}$$

$$\textit{The balance of forces:} \qquad F_c = F_{st} \cos\alpha \tag{20}$$

$$\textit{The balance of moments:} \qquad M = F_c \left(r_h - c_s - \frac{\lambda x}{2} \right) \tag{21}$$

where E_s is the Young's modulus of steel and ε_s is the average strain of the reinforcements, which can be computed by:

$$\frac{\varepsilon_{cu}}{x} = \frac{\varepsilon_t}{r_h - x} \tag{22}$$

$$\frac{\varepsilon_s}{r_h - c_s} = \frac{\varepsilon_t \cos\alpha}{r_h} \tag{23}$$

The required reinforcement area, A_{st} in this case, can be generated by solving the force equilibrium equations above:

$$A_{st} = \frac{D_d \lambda x^2 f_{cd}}{2E_s \varepsilon_{cu} \left(rh - x \right) \cos\alpha} \tag{24}$$

in which x is the depth of the neutral axis calculated by:

$$x = \frac{-D_d \cos\alpha \lambda f_{cd} \left(r_h - c_s \right) + \sqrt{\left[D_d \cos\alpha \lambda f_{cd} \left(r_h - c_s \right) \right]^2 - 2MD_d \cos\alpha \lambda^2 f_{cd}}}{-D_d \cos\alpha \lambda^2 f_{cd}} \tag{25}$$

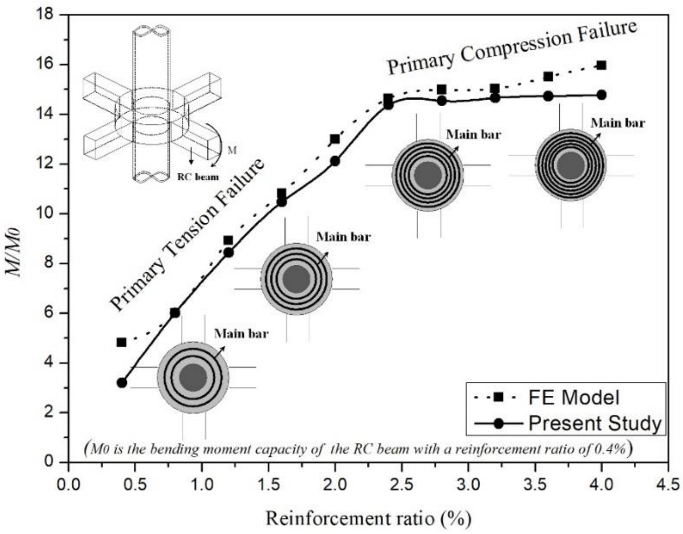

Figure 16 The results from the FEA and the proposed design equation for failure mode B

A series of SCCR joints with different reinforcement ratios are analysed by the FEA method to ensure the accuracy of the equations proposed above. The results from both the FE model and the hand calculations are shown in Figure 16. It is evident that both the failure moment of the *Primary Tension Failure* and the *Primary Compression Failure* can be accurately predicted using the equations proposed in this paper.

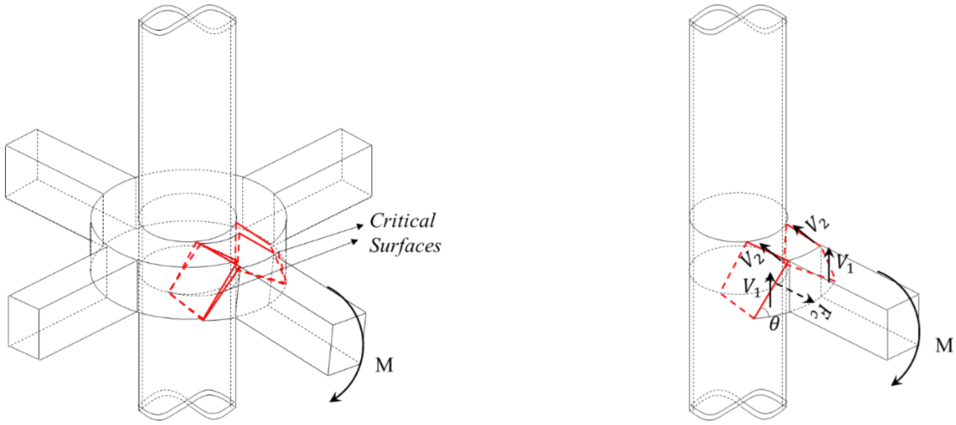

(a) (b)

Figure 17 Torsional failure of the ring beam

3.3 Failure Mode C - Torsional Failure of the Ring Beam

The potential failure surfaces of this failure mode and the torsion-resistant forces on the failure surfaces are shown in Figure 17 (b), in which V_1 and V_2 are the resistant forces from the hoop bars of the ring beam and Fc is the compression force which can be calculated by equations (12) or (18). The force equilibrium equations of the critical surfaces can be written as:

$$M = 2V_1 \frac{b_{cor}}{2} + 2V_2 \frac{r_{hcor}}{2} + \beta F_c \left(\frac{r_h}{2} - \frac{\lambda x}{2} \right) \tag{26}$$

where $\beta=0.83$ is a reduction factor generated from parametric studies and r_{hcor} and b_{cor} are the effective depth and width of the ring beam as shown in Figure 18.

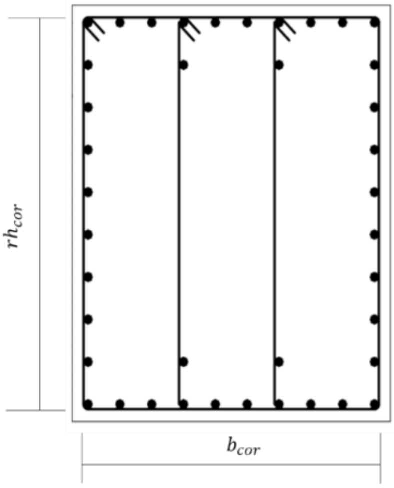

Figure 18 The definitions of r_{hcor} and b_{cor}

By assuming the hoop bars and side bars crossing the cracking lines yield when the joint fails in torsion, the forces on the cracking lines will be as shown in Figure 19.

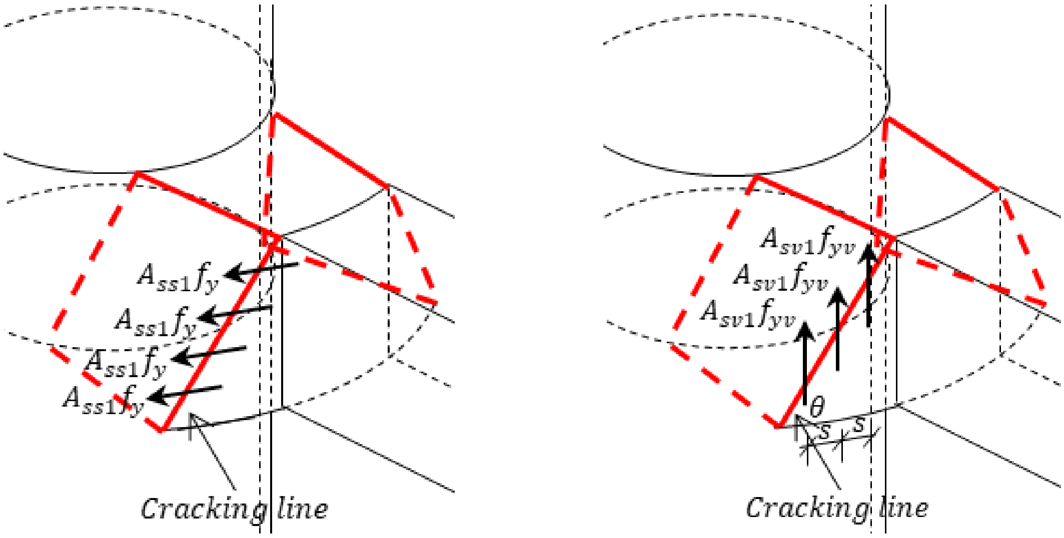

(a) The resistant forces from the side bars (b) The resistant forces from the hoop bars

Figure 19 The forces on the lines of potential crack

From Figure 19 (b), the resistant forces from the hoop bars V_1 and V_2 can be calculated by:

$$V_1 = \frac{A_{sv1} r_{hcor} \cot\theta f_{sv}}{s} \tag{27}$$

$$V_2 = \frac{A_{sv1} b_{cor} \cot\theta f_{sv}}{s} \tag{28}$$

in which A_{sv1} is the area of one leg of the hoop bar, s is the spacing of the hoop bars, f_{sv} is the yield strength of hoop bars, and θ=45° is the angel between the cracking lines and the axis of the ring beam as shown in Figure 19 (b).

By substituting equations (27) and (28) into (26), the twisting moment capacity is generated and shown by:

$$M = 2\frac{A_{sv1} r_{hcor} b_{cor} \cot\theta f_{sv}}{s} + \beta F_c \left(\frac{r_h}{2} - \frac{\lambda x}{2} \right) \tag{29}$$

Since the twisting moment is primarily carried by the outermost hoop bars, the recommended layouts of the hoop bars are shown in Table 1.

Table 1 Layouts of the hoop bars and the corresponding factors

n	*Layouts*	η
n=1	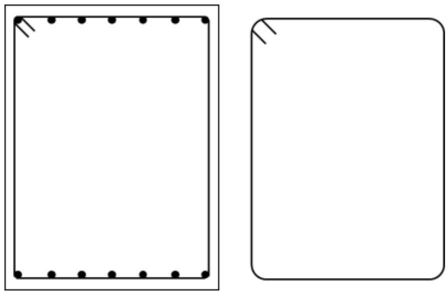	$\eta=1$
n=2	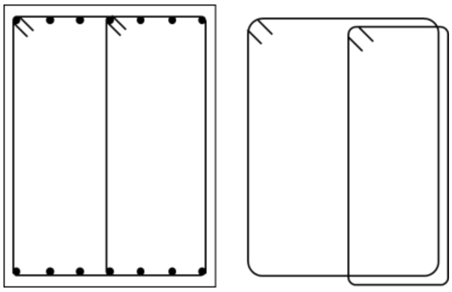	$\eta=1.8$
n=3	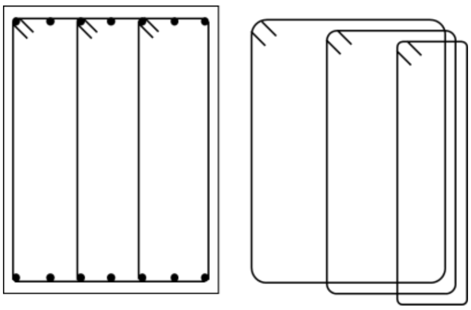	$\eta=2.4$

For different layouts of the hoop bars, equation (29) should be modified as:

$$M = 2\eta \frac{A_{sv1} r h_{cor} b_{cor} \cot\theta f_{sv}}{s} + \beta F_c \left(\frac{rh}{2} - \frac{\lambda x}{2} \right) \tag{30}$$

where η is the factor shown in Table 1.

The relationship between the resistant forces from the side bars and those from the hoop bars is:

$$\sum A_{sv1} f_{sv} \cot\theta = \sum A_{ss1} f_{yd} \tag{31}$$

where

$$\sum A_{sv1} f_{sv} = n \frac{rh_{cor} \cot\theta}{s} A_{sv1} f_{sv} \tag{32}$$

in which n is the number of closed links as shown in Table 1, A_{ss1} is the area of one side bar, and the required number of side bars in one side is：

$$m = n \frac{rh_{cor} \left(\cot\theta\right)^2}{s} \frac{A_{sv1} f_{sv}}{A_{ss1} f_{yd}} \tag{33}$$

Three groups of SCCR joints with different hoop bar layouts are analysed using the FEA method and the equations proposed above, and the results are shown in Figure 20. These figures show that the joint capacities produced by the proposed equations are accurate.

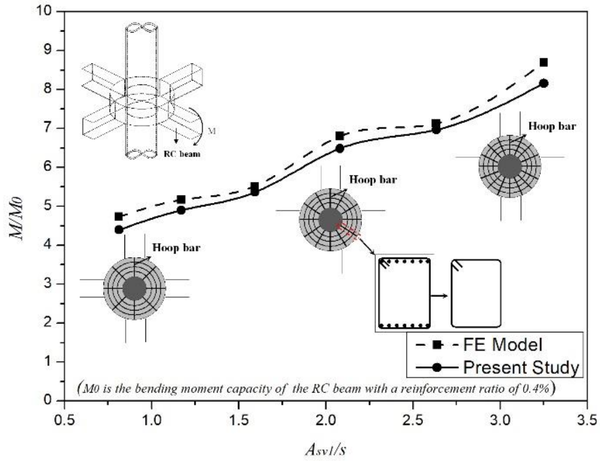

(a) *n=1*

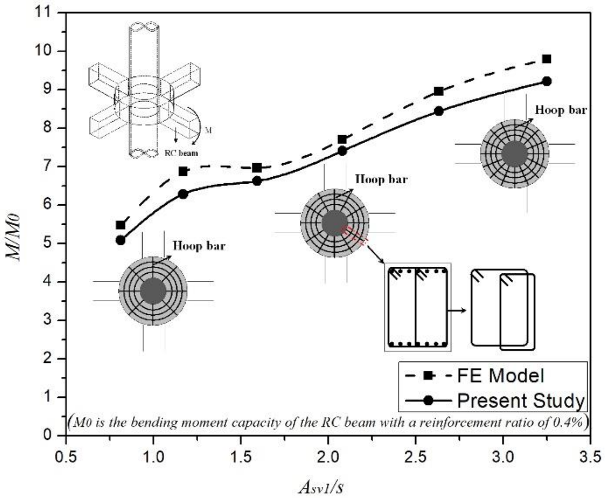

(b) *n=2*

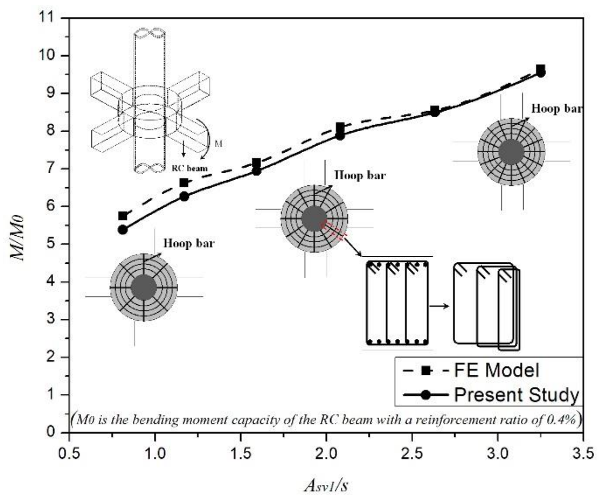

(c) *n=3*

Figure 20 The results from FEA and the proposed design equations for failure mode C

3.4 Failure Mode D - Failure of the Shear Studs

Results from the FE model show that the SCCR joint might also fail due to the failure of shear studs as shown in Figure 21. To prevent this kind of failure mode, the number of shear studs should be calculated by:

$$n_s = \frac{\Sigma V_i}{p_V} \tag{34}$$

in which p_v is the design shear capacity of a shear stud.

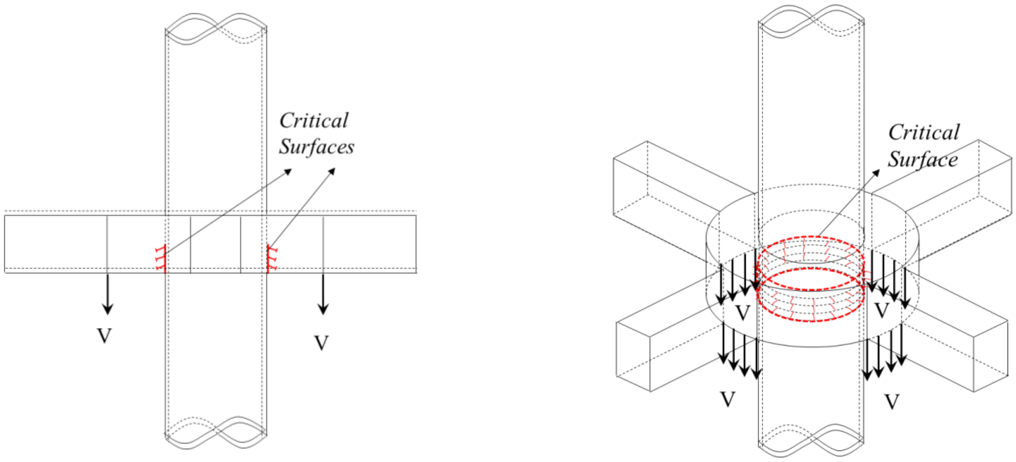

Figure 21 The failure of the shear studs

All the shear studs should be placed uniformly along the perimeter of the steel tube in compression regions. For considering locally concentrated shear forces from the adjacent beam, the following checking is also required:

$$\frac{n_s}{4} \geq 0.5 \frac{\max(V_i)}{p_V} \tag{35}$$

4 Design Procedure

Drawing on the aforementioned failure modes and corresponding design equations, the detailed SCCR joints design procedure is illustrated in Figure 22. The process begins with the determination of the maximum moment M, the unbalanced moment M_u, and all the shear forces

V_i applied on the SCCR joint. Next, the width of the ring beam is determined. According to parametric studies, the ring beam width is not a critical parameter that directly affects the failure modes; however, a width of 1.0 to 1.4 times that of the RC beam should be provided. In addition, the required ring beam height should be calculated using equation (3). It should be noted that the SCCR joints are much larger than the SPSC joints, so a larger amount of space will be taken up by the RC ring beam. Thus, the acceptability of the ring beam size is a factor that should be carefully considered before the next step.

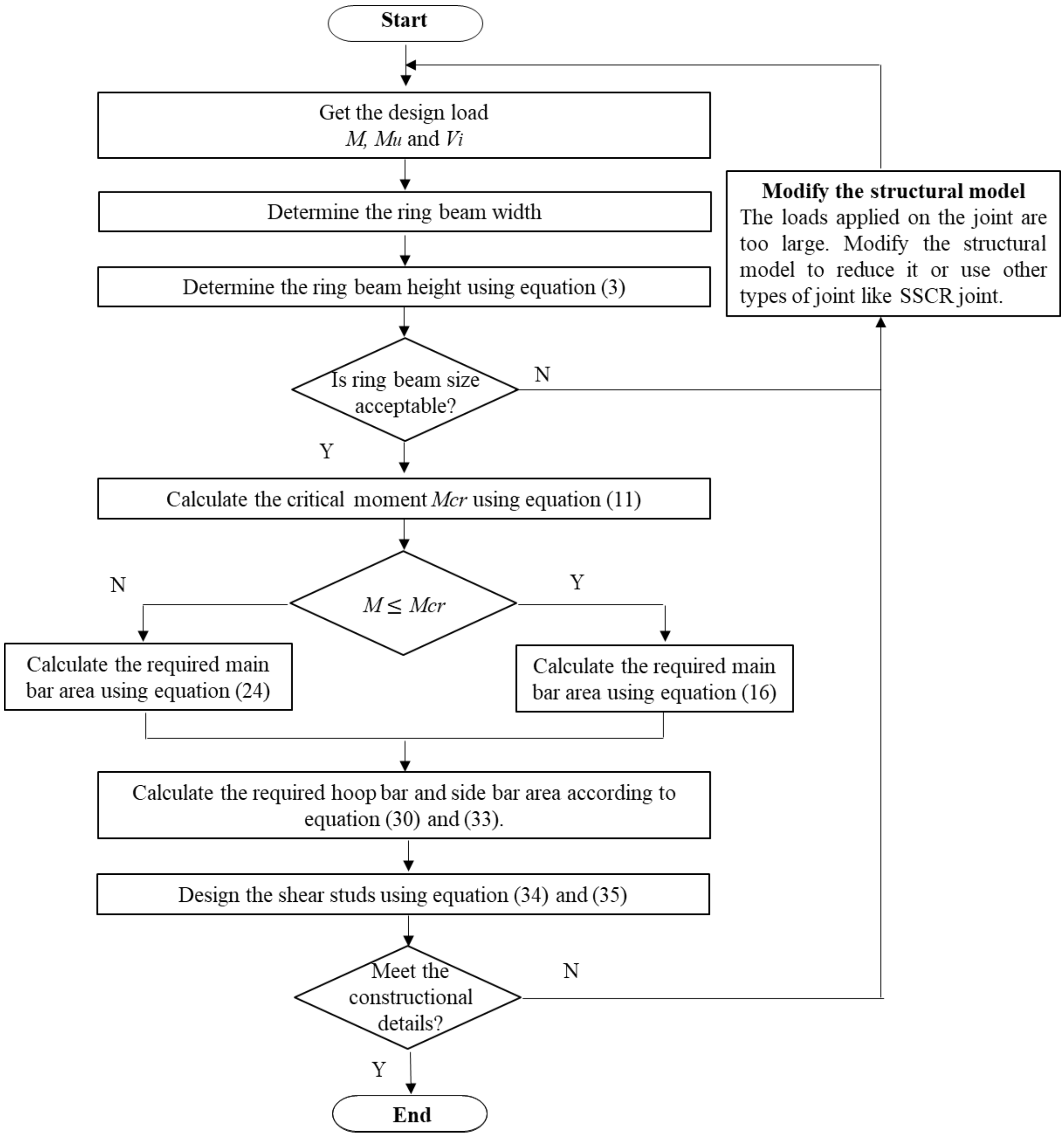

Figure 22 Design procedure

After determining the ring beam size, the required main bar area can be designed using equation (16) or (24), and the required hoop bar and side bar areas can be calculated according to equation (30) and (33). Shear studs can be checked for adequacy of strength using equations (34) and (35).

Furthermore, recommendations for the design of the SCCR joint are:

- the section height of the ring beam should be no less than that of the adjacent RC beam;
- the area of the top bar and bottom bar of the ring beam should be larger than that of the adjacent RC beam; and,
- the shear studs should be placed uniformly along the perimeter of the steel tube in compression regions.

5 An Example

A real-world project in Hong Kong has been completed according to the design equations proposed above. In this project, a building was constructed using the reverse construction method, and the SCCR joints were employed to connect the bored piles and ground beams at floors B1 and B2. Overall, approximately thirty SCCR joints were designed. The diameters of the bored pile vary from 2.0m to 3.2m, and each pile consisted of three or four connected ground beams. One of the SCCR joints was selected and designed according to the detailed design procedure shown below, with the result being further validated by the FEA.

5.1 Design Procedure

Both the geometric and loading information of the joint and the design procedure based on the proposed equations are shown in Table 2. Concrete and reinforcement steel with the grade of C45 and S500 were used in this project, and the material properties were taken from the local design code [29].

Table 2 Design procedure

	1	*2*	*3*	*4*
M (kNm)	4000	4000	0	4000
V (kN)	2000	1000	0	4000

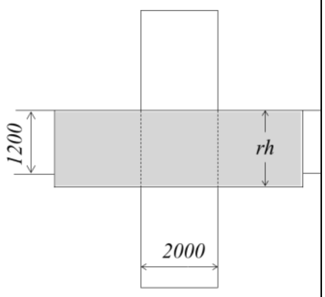

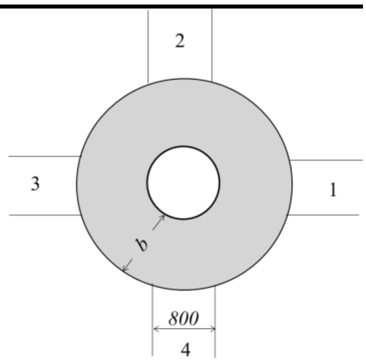

Determine the size of ring beam based on *Failure mode A*	A width of 1.0 times the ground beam was adopted: b=800mm； Calculate the required ring beam height using equation (3): $M_u = \frac{\alpha\pi d}{2}\frac{\sigma_{bc}}{2}\frac{r_h}{2}\frac{2r_h}{3}$ → r_h=717mm<1200mm **Choose** the ground beam height as the ring beam height: r_h=1200 mm
Calculate the required main bar based on *Failure mode B*	Calculate the critical moment M_{cr} using equation (11): $M_{cr}=18778kNm$ *M=4000kNm<M’,* find the required main bar area and the depth of the neutral axis with equation (16) and (17): $A_{st}=4697mm^2$； x=98mm **Given** 6 number of Φ32 reinforcement bars (*Ast=4823mm2*) as the main bar of the RC ring beam.
Calculate the required hoop bar and side bar based on *Failure mode C*	Choose the hoop bar layouts as the second row of Table 1 with two close links (*n=2* and *η=1.8).* Calculate the required hoop bar area with equation (30): $A_{sv1}/s=1.42mm$ **Given** Φ14 hoop bars with the spacing of 100mm ($A_{sv1}/s=1.54mm$). Calculate the required side bar area with equation (33):

	A_{ss} =3207mm^2 **Given** 8 Φ25 reinforcement bars on each side (*Ast=3925mm2*)
Design the shear studs based on *Failure mode D*	Using shear studs with 19mm diameter, and the design shear capacity of one shear studs is p_v=81.68kN Calculate required number of shear studs with equation (36): $n = \frac{V_1 + V_2 + V_3 + V_4}{p_v} = 123$ **Given** 6 rows of shear studs with 22 shear studs in each row Check: $\frac{n}{4} = 33 \geq 0.5 \frac{V_{max}}{p_v} = \frac{4000}{81.68} \times 0.5 = 24.5$, OK!
Reinforcement details	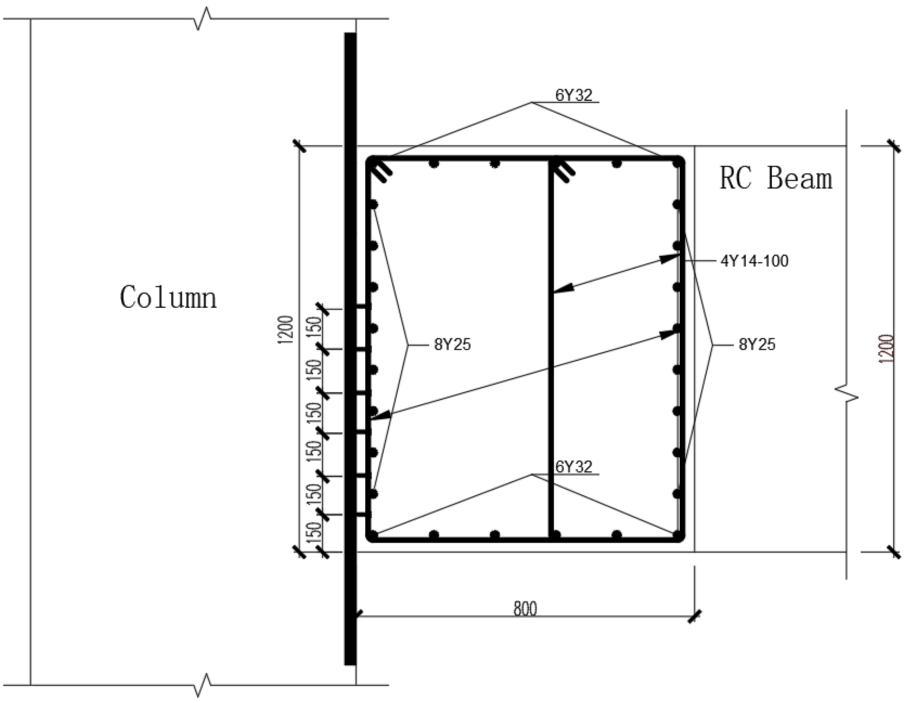

379

5.2 Validation by FEA

To validate the accuracy of the proposed design equations, the FE model for the SCCR joint designed above is established as given in Figure 23, and the analysis results are shown in Figure 24. The FEA results shown in Figure 24 illustrate that no component is over-stressed and that the joint has enough strength capacity to resist the applied load.

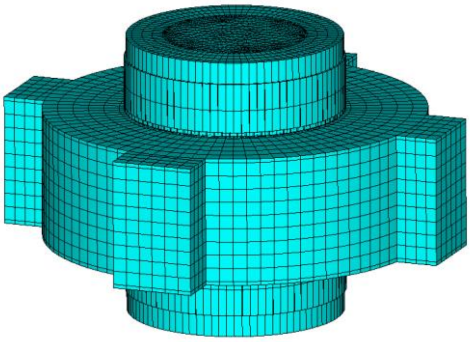

Figure 23 FE Model

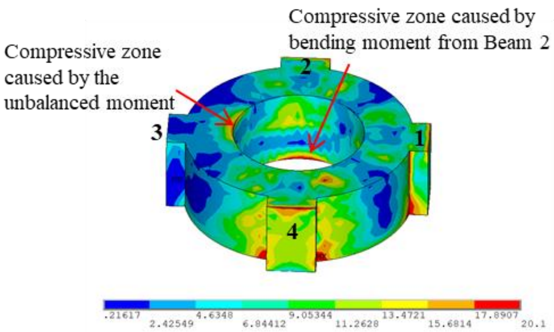

(a) Stress contour of the ring beam (Unit: N/mm2)

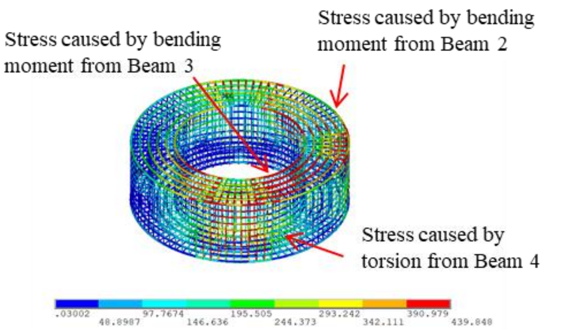

(b) Stress contour of the reinforcement (Unit: N/mm2)

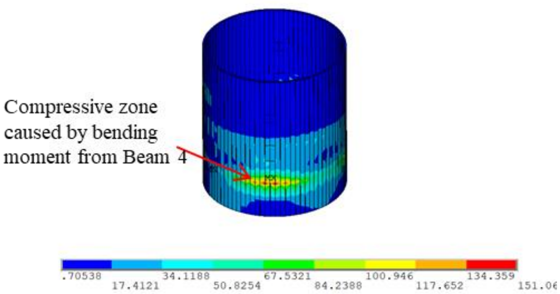

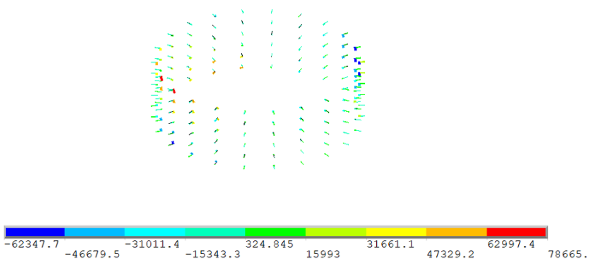

Max:78.67$kN < p_v = 81.68kN$

(c) Stress contour of the steel tube (Unit: N/mm2)

(d) Shear forces of shear studs (Unit: N)

Figure 24 FEA results

6 Conclusion

This paper develops a sophisticated FE model for SCCR joints wherein the dominant factors affecting the joint's performance are considered. From the FEA results, four possible failure modes are identified: A) bearing crushing of the ring beam concrete, B) bending failure of the ring beam, C) torsional failure of the ring beam, and D) failure of the shear studs. Based on the modern joint design process in Eurocode-3-1-8 [14], design equations for computing the SCCR joint's strength in regard to the failure modes are proposed. The parametric studies have been conducted to derive these design equations. Finally, a design example from a real-world construction project is presented using the proposed equations.

7 Acknowledgments

The first and the last authors are grateful for financial support from the Research Grant Council of the Hong Kong SAR Government on the project "Joint-based second order direct analysis for domed structures allowing for finite joint stiffness (PolyU 152039/18E)". The second author would like to express his gratitude to Sun-Yat-Sen University on the "Early Research Career Scheme Grant (76140-18831105)".

Appendix-I – Calculation of the Unbalanced Moment

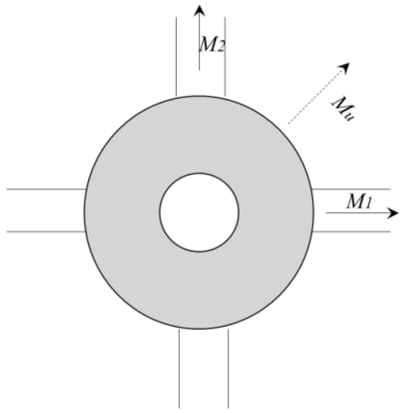

Figure 25 Moments applied on an SCCR joint

This paper defines the vector sum of the moments applied on an SCCR joint as *the unbalanced moment.* This unbalanced moment is the moment transferred by the SCCR joint from the beams to the column. Two moments (M_1 and M_2) are applied on an SCCR joint as shown in Figure 25, and the unbalanced moment caused by this can be calculated by:

$$M_u = \sqrt{{M_1}^2 + {M_2}^2} \tag{36}$$

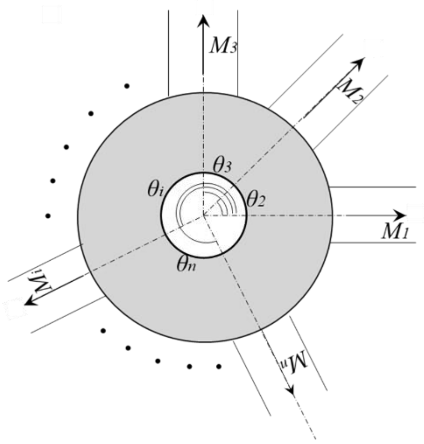

Figure 26 Moments applied on an SCCR joint (general case)

For the general case as shown in Figure 26, the unbalanced moment can be computed by:

$$M_u = \sqrt{\left(\sum_{i=1}^{n} M_i \cos\theta_i\right)^2 + \left(\sum_{i=1}^{n} M_i \sin\theta_i\right)^2} \tag{37}$$

References

[1] Han, L.-H., W. Li, and R. Bjorhovde, Developments and advanced applications of concrete-filled steel tubular (CFST) structures: Members. Journal of Constructional Steel Research, 2014. 100: p. 211-228.

[2] Lee, C.-H., J.-W. Kim, and J.-G. Song, Punching shear strength and post-punching behavior of CFT column to RC flat plate connections. Journal of Constructional Steel Research, 2008. 64(4): p. 418-428.

[3] Kim, J.-W., C.-H. Lee, and T.H. Kang, Shearhead reinforcement for concrete slab to concrete-filled tube column connections. ACI Structural Journal, 2014. 111(3): p. 629.

[4] Schneider, S.P. and Y.M. Alostaz, Experimental behavior of connections to concrete-filled steel tubes. Journal of Constructional Steel Research, 1998. 45(3): p. 321-352.

[5] Elremaily, A. and A. Azizinamini, Design provisions for connections between steel beams and concrete filled tube columns. Journal of Constructional Steel Research, 2001. 57(9): p. 971-995.

[6] Cheng, C.-T. and L.-L. Chung, Seismic performance of steel beams to concrete-filled steel tubular column connections. Journal of Constructional Steel Research, 2003. 59(3): p. 405-426.

[7] Ricles, J., S. Peng, and L. Lu, Seismic behavior of composite concrete filled steel tube column-wide flange beam moment connections. Journal of Structural Engineering, 2004. 130(2): p. 223-232.

[8] Sheet, I.S., U. Gunasekaran, and G.A. MacRae, Experimental investigation of CFT column to steel beam connections under cyclic loading. Journal of Constructional Steel Research, 2013. 86: p. 167-182.

[9] Azizinamini, A., Y. Shekar, and M.A. Saadeghvaziri, Design of through beam connection detail for circular composite columns. Engineering structures, 1995. 17(3): p. 209-213.

[10] Tang, X.-L., et al., Seismic behaviour of through-beam connection between square CFST columns and RC beams. Journal of Constructional Steel Research, 2016. 122: p. 151-166.

[11] Nie, J., Y. Bai, and C. Cai, New connection system for confined concrete columns and beams. I: Experimental study. Journal of Structural Engineering, 2008. 134(12): p. 1787-1799.

[12] Bai, Y., J. Nie, and C. Cai, New connection system for confined concrete columns and beams. II: theoretical modeling. Journal of Structural Engineering, 2008. 134(12): p. 1800-1809.

[13] Zhang, Y., J. Zhao, and C. Cai, Seismic behavior of ring beam joints between concrete-filled twin steel tubes columns and reinforced concrete beams. Engineering Structures, 2012. 39: p. 1-10.

[14] The European Committee for Standardization, Eurocode 3: Design of steel structures—Part 1-8: Design of joints. 2005.

[15] Bijlaard, F., Eurocode 3, a basis for further development in joint design. Journal of Constructional Steel Research, 2006. 62(11): p. 1060-1067.

[16] D'Aniello, M., et al., Seismic design of extended stiffened end-plate joints in the framework of Eurocodes. Journal of Constructional Steel Research, 2017. 128: p. 512-527.

[17] El-Khoriby, S., et al., Modelling and behaviour of beam-to-column connections under axial force and cyclic bending. Journal of Constructional Steel Research, 2017. 129: p. 171-184.

[18] Subramani, T., et al., Finite Element Modeling On Behaviour Of Reinforced Concrete Beam Column Joints Retrofitted With CFRP Sheets Using Ansys. International Journal of Engineering Research and Applications, 2014. 4(12): p. 69-76.

[19] Ramadan, H.M., et al., Finite element analysis of circular concrete filled tube connections. Journal of Constructional Steel Research, 2016. 120: p. 33-44.

[20] Ouyang, Y., et al., Finite element analysis of concrete-filled steel tube (CFST) columns with circular sections under eccentric load. Engineering Structures, 2017. 148: p. 387-398.

[21] Ouyang, Y. and A. Kwan, Finite element analysis of square concrete-filled steel tube (CFST) columns under axial compressive load. Engineering Structures, 2018. 156: p. 443-459.

[22] Pagoulatou, M., et al., Finite element analysis on the capacity of circular concrete-filled double-skin steel tubular (CFDST) stub columns. Engineering Structures, 2014. 72: p. 102-112.

[23] Friedman Z, Kosmatka J B. An improved two-node Timoshenko beam finite element. Computers & structures, 1993, 47(3): 473-481.

[24] Hutchinson J R. Shear coefficients for Timoshenko beam theory. Journal of Applied Mechanics, 2001, 68(1): 87-92.

[25] Johnson, R. and I. May, Partial-interaction design of composite beams. Structural Engineer, 1975. 8(53).

[26] The European Committee for Standardization, Eurocode 4: design of composite steel and concrete structures. 1994: CEN.

[27] Lam, D. and E. El-Lobody, Behavior of headed stud shear connectors in composite beam. Journal of Structural Engineering, 2005. 131(1): p. 96-107.

[28] Shim, C.-S., P.-G. Lee, and T.-Y. Yoon, Static behavior of large stud shear connectors. Engineering Structures, 2004. 26(12): p. 1853-1860.

[29] Building Department, Code of practice for structural use of concrete 2013. 2013, The HKSAR Government Hong Kong.